# Divergent visual ecology of *Drosophila* species drives object-tracking strategies matched to landscape sparsity

#### **Highlights**

- Related species often have vastly visual ecological constraints
- Drosophila species from different visual habitats show divergent visual behaviors
- D. melanogaster use a "ground-fixate, object-saccade" strategy to track objects
- D. mojavensis use a fused fixate-and-saccade strategy to track objects

#### **Authors**

Martha Rimniceanu, Daniela Limbania, Sara M. Wasserman, Mark A. Frye

#### Correspondence

frye@ucla.edu

#### In brief

Related species can have different visual ecology. Rimniceanu et al. show that desert *Drosophila* species adapt their flight control to combine smooth pursuit and saccades to track sparse visual features of the landscape. Cosmopolitan flies fix their gaze on the cluttered visual background and then track objects with saccades.







#### **Article**

# Divergent visual ecology of *Drosophila* species drives object-tracking strategies matched to landscape sparsity

Martha Rimniceanu, Daniela Limbania, Sara M. Wasserman, and Mark A. Frye<sup>1,3,\*</sup>

<sup>1</sup>Department of Integrative Biology and Physiology, University of California, Los Angeles, Los Angeles, CA 90095, USA

\*Correspondence: frye@ucla.edu

https://doi.org/10.1016/j.cub.2024.08.036

#### **SUMMARY**

Maintaining stable gaze while tracking moving objects is commonplace across animal taxa, yet how diverse ecological needs impact these processes is poorly understood. During flight, the fruit-eating fly Drosophila melanogaster maintains course by making smooth steering adjustments to fixate the image of the distant visual background on the retina, while executing body saccades to investigate nearby objects such as food sources. Cactophilic Drosophila mojavensis live where there is no canopy; rather, the flora forming visual "background" and "objects" are one and the same. We tested whether D. mojavensis have adapted their flight control strategies for a visually sparse landscape. We used a magnetic tether that allows free movement in the yaw axis. In response to a textured bar moving across a similarly textured stationary background, D. melanogaster fixates the background, thereby stabilizing gaze while integrating bar dynamics to trigger tracking saccades. By contrast, two mojavensis subspecies in the repleta subgroup and one species in the melanogaster subgroup steer to smoothly fixate the bar, seemingly ignoring the stationary surround. Desert flies execute frequent bar-tracking saccades, but theirs are triggered when rotational velocity lags the bar. Thus, D. melanogaster, which lives in visually cluttered cosmopolitan habitats, leverages the optical disparities between nearby objects and distant foliage for a hybrid control strategy: "ground-fixate, objectsaccade." Flies in distant phylogenetic subgroups with similar visual ecology use a "fixate-and-saccade" strategy, which would be adaptive in a visually sparse environment where individual landscape features are both approached and used to maintain a straight course.

#### **INTRODUCTION**

The visual landscapes that locomoting animals encounter often consist of spatially complex and dynamical features. Coherent motion of the panorama subtending a large portion of the total visual field, so-called "wide-field" motion, is generated by self-movement against distant visual clutter and engages ubiquitous optomotor responses to reduce retinal slip and maintain stable gaze. Fixated gaze allows easy discrimination of the relative movement dynamics of nearby features or objects that subtend a narrow region of the visual field, so-called "small-field" stimuli, which generally represent navigational goals. For example, a fly cruising through a forest might fixate the panoramic image of distant background foliage to maintain a stable course, while the movement disparity generated by the image of a nearby tree trunk evokes a steering maneuver. But, what if the visual environment is sparse, consisting of a single tree on an open horizon? Would this feature drive both optomotor gaze fixation and object navigation?

Differences between the retinal size and movement dynamics of wide-field and small-field cues have provided a classical conceptual framework to analyze flight control strategies and visual processing circuits in flies. More recently, the widely used model system *Drosophila melanogaster* has provided much of our emerging understanding of visual flight control and the cellular mechanisms of motion vision and feature detection. Melanogaster originated in sub-Saharan Africa and radiated outward, starting 10,000 years ago, to colonize essentially all niches where climate conditions are favorable. Description melanogaster is an ecological generalist that is part of the "cosmopolitan guild" of the Sophophora subgenus of *Drosophila*, feeding and breeding on varied decomposing fruit matter, which contributes to their success in diverse environments 9,10

As a human commensal, *D. melanogaster* is adapted to generic cluttered visual environments, ranging from forests to cityscapes. Such ecologies present a complex figure-ground discrimination challenge as they are largely composed of vertically elongated features that define both the distant panoramic background and nearby objects. In the face of this sensory challenge, *D. melanogaster* has evolved a hybrid control strategy in which wide-field motion engages smooth optomotor gaze fixation, which is interspersed with nystagmus or catch-up



<sup>&</sup>lt;sup>2</sup>Department of Neuroscience, Wellesley College, Wellesley, MA 02481, USA

<sup>&</sup>lt;sup>3</sup>Lead contact





saccades,<sup>3</sup> whereas nearby small-field objects trigger course-changing body saccades while optomotor responses are suppressed. <sup>11,12</sup> Smooth optomotor corrections rely upon directionally selective motion-detecting neurons called T4 and T5, <sup>13</sup> whereas object-tracking body saccades are mediated by T3 feature detectors. <sup>14,15</sup> Thus, during flight, *D. melanogaster* elegantly maps visual features to distinct visual control algorithms.

However, not all visual landscapes are densely cluttered. By contrast to cosmopolitan D. melanogaster, D. mojavensis evolved within visually sparse desert landscapes. Separated from D. melanogaster by nearly 40 million years, these members of the repleta subgroup first radiated in South America and specialized on fermenting cacti. 16,17 Today, four geographically separated subspecies comprise the D. mojavensis species. Within these, D. moj. baja and D. moj. mojavensis are hypothesized to have diverged approximately 250,000 years ago and specialize on agria cacti (Stenocereus gummosus) and barrel cacti (Ferocactus cylindraceus), respectively. 16,18,19 The host cacti of both subspecies are native to bright, barren Mojave and Baia desert environments, where the fewer vertical features available comprise both wide-field panoramic cues and smallfield landscape features representing food and breeding sites. Presumably driven by their distinct visual habitats, D. melanogaster approach vertical bars or edges that likely represent landscape features while avoiding small objects presumably resembling approaching predators, whereas cactophilic desert-dwelling D. mojavensis are attracted to objects of any size.<sup>20</sup> A comparative approach requires analysis of another species to differentiate between visual ecology and phylogenetic mechanisms. Drosophila vakuba resides in the melanogaster subgroup, yet, unlike D. melanogaster, inhabits the canopyfree sparse landscape of the African savannah.

Motivated by their different visual ecologies, we tested the hypothesis that the control strategies for gaze stabilization and object tracking have diverged between cosmopolitan and desert drosophilids. We characterized flight-steering responses to a camouflaged vertical bar, which is observable only while it is moving, during tethered, yaw-free flight by D. melanogaster, D. moj. baja, and D. moj. moj. Surprisingly, desert-adapted species smoothly fixate and then center the bar on their visual midline, whereas fixation movements in yaw-free D. melanogaster are absent, although some lab strains saccade toward the object more readily than others. The smooth fixation dynamics of desert flies are similar to responses to wide-field motion and result in bar centering on the visual midline. For objects that move along a continuous path, saccadic pursuit ensues in all three species, albeit with species-specific dynamics. In direct contrast to D. melanogaster, and more akin to primate visual pursuit, desert flies rely heavily on both smooth fixation dynamics and catch-up saccades to track a moving object, triggering saccades when object velocity is high. Results from phylogenetically distant species with similar visual ecology support the hypothesis that a sparse visual landscape promotes the fused control of gaze stabilization and object pursuit. Our findings build upon previous work showing contextual modulation of object-pursuit behavior and its underlying neural mechanisms<sup>21</sup> within a comparative visual ecological context.

#### **RESULTS**

## Bar-centering behavior varies across strains and species

We compared the visual responses to a vertical object in three lab strains of *D. melanogaster*, two subspecies of *D. mojavensis*, namely D. moj. baja and D. moj. moj., and D. yakuba (Figures 1A and S1A). We presented a bar oscillating ± 30° amplitude at constant velocity on a triangle waveform at random azimuthal locations relative to the fly's visual midline. The moving bar was presented on a stationary, randomly patterned background. The bar was therefore defined only by the relative motion between the bar and background rather than luminance cues that would provide static position information independent from object motion (e.g., a dark bar on a bright background). Our previous work found that transitioning from a rigidly tethered body-fixed state to a magnetically tethered yaw-free body state strongly modulates object orientation responses in D. melanogaster.21 Here, all experiments were conducted in the yaw-free apparatus (Figure 1B).

Regardless of the azimuthal position of the oscillating bar, *D. melanogaster* of the Dickinson lab (DL) strain did not visually orient toward or center the object (Figure 1Ci). Plotting the population data onto a circular probability heatmap showed a uniform likelihood of flies orienting at all angular positions relative to the bar throughout all trials (Figure 1Ci). For repeated trials from each individual fly, we computed an average resultant heading vector, the magnitude of which represents the strength of the average response. A vector magnitude of 1 is equivalent to the fly spending the entire trial at a constant angular heading. In this representation, *D. melanogaster* from the DL strain shows uniformly distributed population responses resulting from generally weak resultant vectors (~0.20) across all individuals (Figure 1Ci).

As visual behavior can vary across lab strains of melanogaster. 22-24 we tested two other lab strains. Canton-S and Oregon-R. Individuals from both strains showed modest centering behavior, although they did not appear to track the bar dynamics, instead making body saccades toward it but increasing their resultant vector (Figures S1Bi-S1Biii). D. moj. baja shows smooth fixation dynamics (Figure 1Cii) and most individuals strongly center the bar (Figure 1Cii). D. moj. moj. displayed similarly strong smooth orientation responses, with all but one fly's resultant vector oriented within 30° of the position of the bar (Figure 1Ciii). Like D. mojavensis, distantly related D. yakuba also strongly orient toward the bar, exemplifying smooth steering dynamics (Figure S1Ciii). Similarly strong resultant vectors (i.e., bar centering) are achieved by different means—in the case of Canton-S and Oregon-R strains of melanogaster by way of saccadic orientation, whereas in the case of D. mojavensis and D. yakuba by way of smooth fixation dynamics.

#### D. mojavensis and D. yakuba smoothly track bar dynamics against a stationary background, unlike D. melanogaster

A study we conducted previously in yaw-free flies showed that whereas *D. melanogaster* responds to wide-field displacements with smooth steering kinematics to stabilize the direction of

#### **Article**



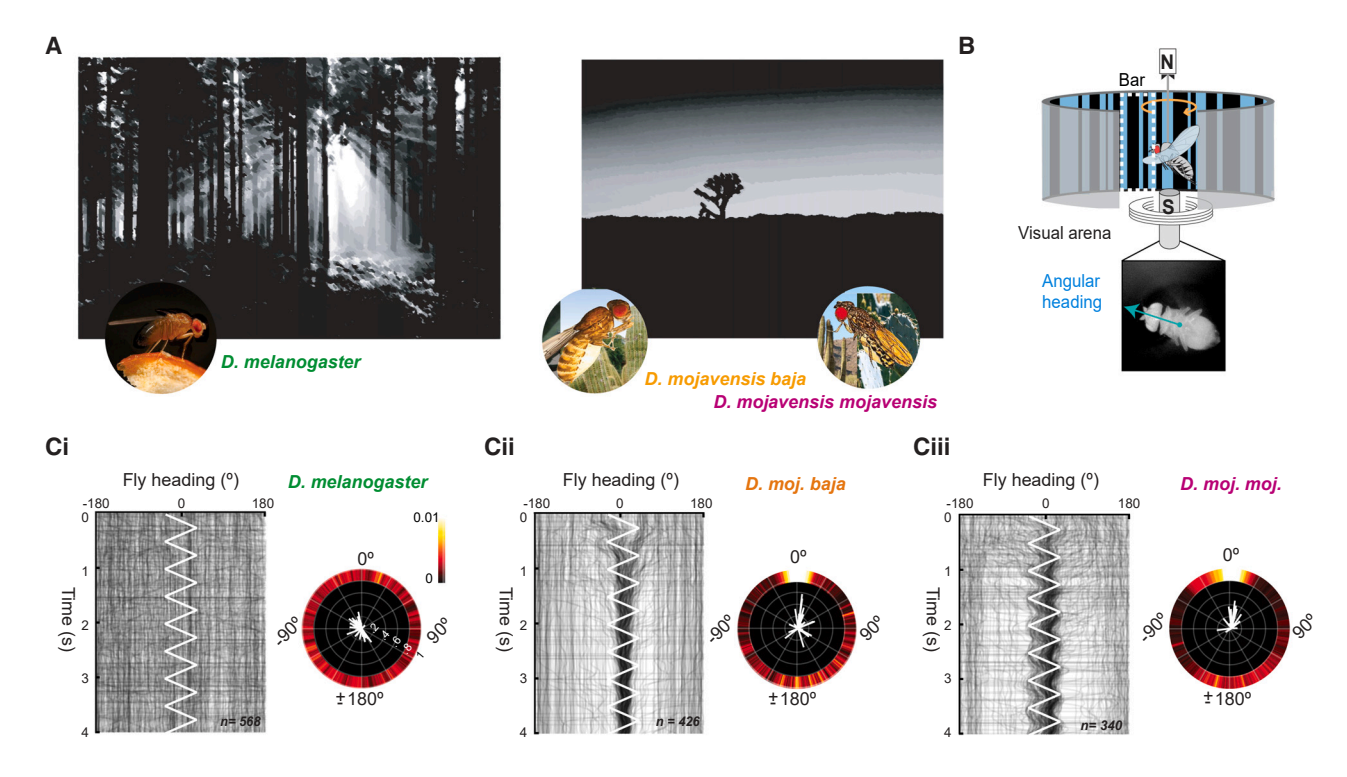


Figure 1. Object centering differs across Drosophila species

(A) Visual scene representing cluttered landscapes inhabited by cosmopolitan generalist *D. melanogaster* and sparse desert landscapes inhabited by *D. moj. baja* and *D. moj. moj.* Monochrome and Gaussian blur filters were applied to both images.

(B) Magnetic tether visual simulator allowing free movement within the yaw plane (orange arrow). A vertical bar of random ON-OFF pixels (white dashed rectangle) on a similar randomly textured background (ON or OFF vertical lines vary in width from 3.75° to 12°). Inset shows a single video frame recorded from below, with the major body axis (cyan vector).

(Cii) Same as (Ci), but for n = 426 trials from N = 20 D. moj. baja.

(Ciii) Same as (Ci), but for n = 340 trials from N = 16 *D. moj. moj.* See also Figure S1.

gaze, they track visual objects primarily with saccades. Rigidly tethered body-fixed flies steer smoothly to follow the dynamics of object motion, but when magnetically tethered, with intact yaw proprioceptive feedback, smooth tracking is strongly attenuated under any stimulus condition but particularly for a motion-defined bar. In a surprising contrast to *D. melanogaster DL*, both *D. moj. baja* and *D. moj. moj.* dynamically fixate a motion-defined bar (Figures 1Cii and 1Ciii). This is impressive because, for an animal to fixate the 30° bar, it must essentially reject the reafferent movement of the 330° visual background.

We adopted the same approach we used previously to quantify smooth steering responses in the desert-dwelling Drosophila species; a motion-defined bar was moved at a fixed velocity (120°/s) and fixed oscillation frequency (2 Hz), initially positioned at  $-60^\circ$ ,  $0^\circ$ , or  $60^\circ$  from the fly's longitudinal midline at the start of each trial (Figure 2A). Positioning the bar at defined egocentric positions was accomplished with real-time heading measurements (see STAR Methods). We also tested responses to the randomly textured wide-field background moved on the same motion trajectory. Under these conditions, none of the three

D. melanogaster strains we tested produce robust smooth steering responses to the bar but clearly fixate the wide-field visual ground (Figures 2Bi and \$2Ai-\$2Aiii). By contrast, and rather surprisingly, D. moj. baja smoothly steer to follow the bar trajectory (Figure 2C). D. moj. moj. showed even stronger average bar responses than D. moj. baja, approaching or exceeding the responses to the magnitude of ground responses (Figures 2C and 2D). D. yakuba showed clear bar responses as well, albeit a bit attenuated by comparison to mojavensis (Figure \$2Biii).

We quantified the strength of smooth steering responses by plotting the magnitude component of the fast-Fourier transform (FFT) for both bar and ground responses. As expected and previously demonstrated, whereas the ground response peaks at 2 Hz, the amplitude of the bar response at this frequency was near zero for *D. melanogaster* (Figures 2C and S2C). By contrast, the bar FFT amplitude for *D. moj. baja* was roughly half that of their ground response, and the bar response amplitude was even higher for *D. moj. moj.* (Figure 2C). *D. yakuba* showed slightly lower response gain, yet with discernible bar responses at the driving frequency (Figure S2C). The ratio of bar-to-ground



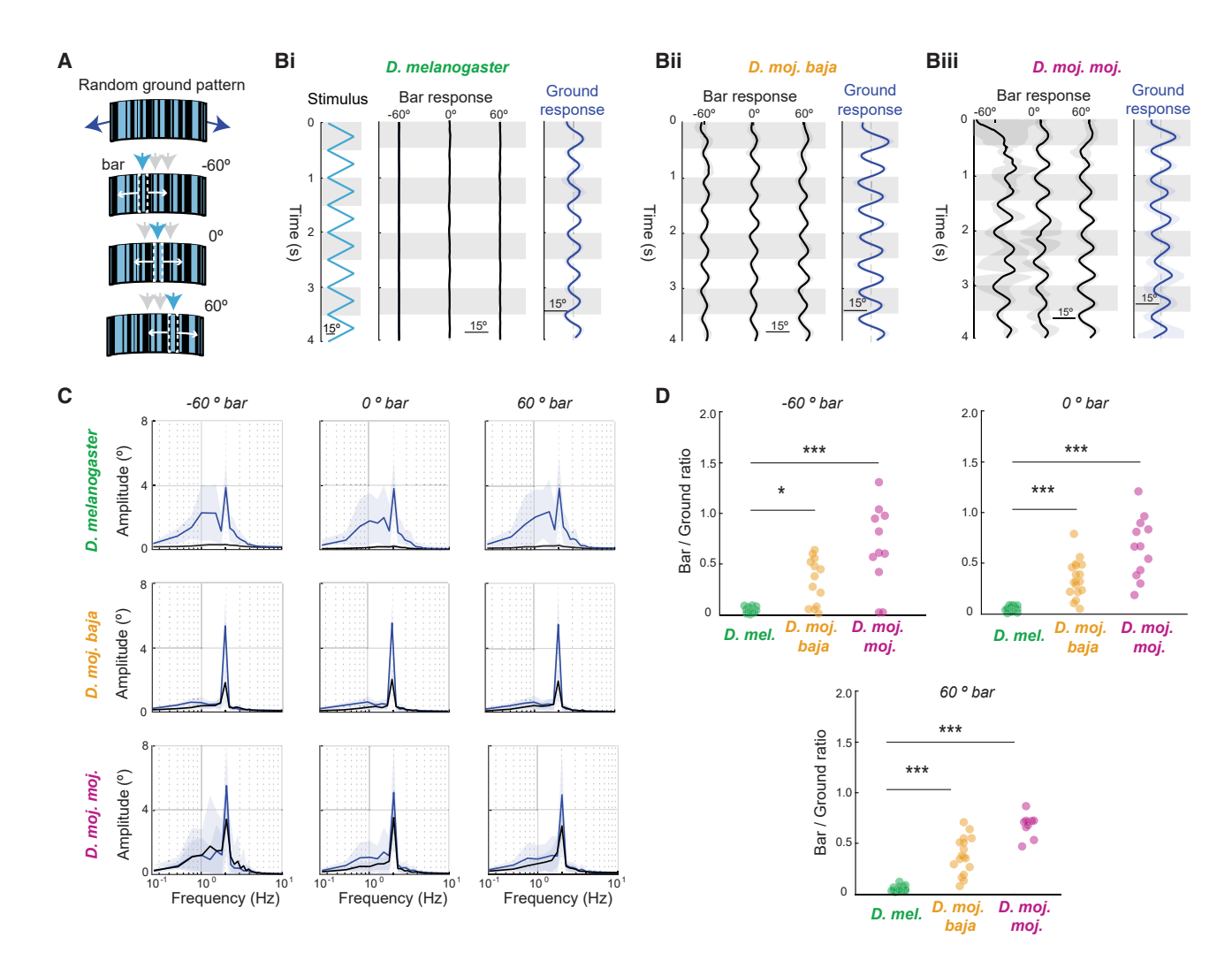


Figure 2. Smooth bar-tracking responses differ for two Drosophila species

(A) Cartoon depiction of 360° randomly textured wide-field ground stimulus and motion-defined small-field bar oscillating about three different initial azimuthal positions relative to the fly's visual midline (blue arrowheads).

(Bi) Mean yaw-free responses to oscillating  $30^{\circ}$  wide bar (black traces) and wide-field ground (dark blue traces) from n = 20 D. melanogaster. Shaded envelopes represent standard deviation of mean. Gray bands highlight alternate stimulus cycles. Saccades were filtered to isolate inter-saccadic bouts in which the bar remains in a constant position relative to the fly's body axis.

- (Bii) Same as (Bi), but for n = 20 D. moj. baja.
- (Biii) Same as (Bi), but for n = 16 D. moj. moj.
- (C) FFT response magnitude to oscillating bar and ground stimuli in the frequency domain. Rows designate species and columns designate initial bar position. Shaded envelopes represent standard deviation of mean.
- (D) Ratio of bar responses to ground responses. Circles represent individual fly means. Unpaired two-sample t tests \*p < 0.05; \*\*p < 0.01; \*\*\*p < 0.001. See also Figure S2.

response amplitudes allows a comparison across species at each of the three azimuthal stimulus positions. Both desert species, *D. moj. baja* and *D. moj. moj.*, as well as *D. yakuba* track bar motion significantly more strongly than all *D. melanogaster* strains, regardless of whether the stimulus is on visual midline or offset to the right or left (Figure 2D; Kruskal-Wallis nonparametric test, Figure S2D). Note that some individual *D. moj. moj.* and *D. yakuba* show bar:ground ratios greater than 1; i.e., the bar, subtending 10% of the visual field, stimulated larger smooth steering responses than the ground, subtending 90% of the visual field. All melanogaster strains tested in the yaw-free state show similarly diminished object fixation behavior, which

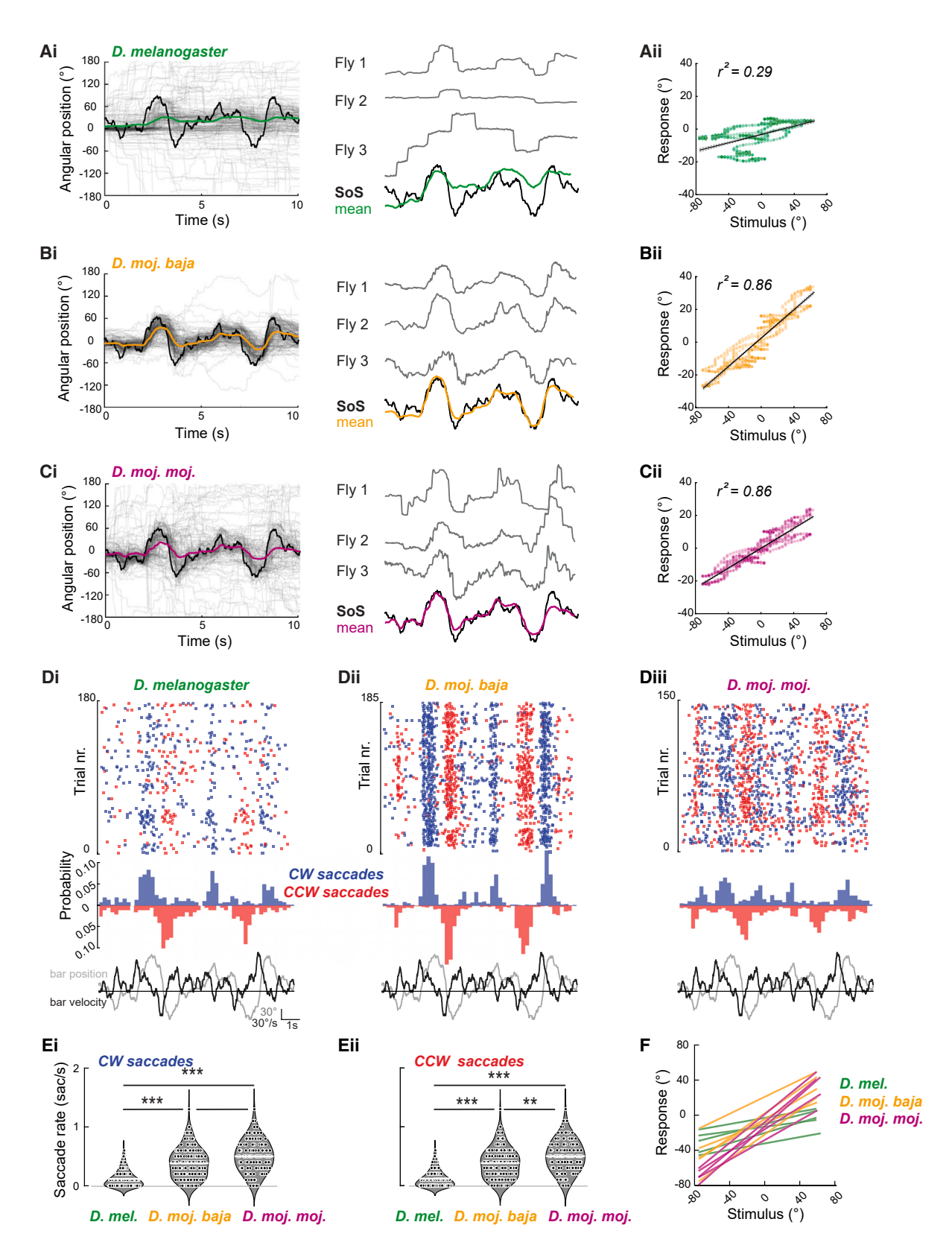
significantly differs from all three desert flies. Thus, from this point onward, we focus our comparison on *D. melanogaster DL* and *D. mojavensis*, which represent divergent bar-tracking strategies seemingly driven by visual ecology rather than phylogeny.

## Distinct from *D. melanogaster*, *D. mojavensis* implement a fixate-and-saccade bar-tracking strategy

Small-field bar and wide-field optomotor responses have long been known to be differentially sensitive to velocity dynamics. Thus, to probe object-centering behavior, the experiments in Figures 1 and 2 were designed to keep image velocity constant,

**Article** 





(legend on next page)



while changing direction twice per second. To explore more naturalistic dynamics, we next designed a complex motion stimulus that comprised nine frequencies spanning a 10-fold range (0.3–11.3 Hz). In addition to eliminating predictability confounds that can occur for constant frequency stimuli, a sum-of-sines (SoS) stimulus can probe the strength of smooth steering responses across a range of frequencies.<sup>26</sup>

Figure 3 shows steering response to the SoS stimulus. At the start of each trial, the bar was centered near the fly's visual midline. As found in prior work, 15,21 D. melanogaster tend to fixate the stationary visual background without smoothly tracking the motion-defined bar, maintaining steady gaze while integrating the positional error of the bar to trigger stepwise tracking saccades (Figure 3Ai). We plotted the SoS stimulus trajectory against the measured mean response values at each time point, which for D. melanogaster indicates that steering responses were only weakly correlated to the SoS stimulus trajectory (Figure 3Aii); the correlation coefficient (r) squared yields the coefficient of determination ( $r^2 = 0.29$ ), indicating that the average D. melanogaster response accounted for merely onethird of variation within the SoS stimulus. Conversely, both desert species showed robust tracking of the SoS stimulus (Figures 3Bi and 3Ci), leading to similarly large r values (0.93) and corresponding r<sup>2</sup> values that explain 86% of the variation within the SoS stimulus (Figures 3Bii and 3Cii). Note that the SoS stimulus evoked seemingly stronger tracking than the single-frequency stimulus (Figure 2). The SoS stimulus is twice the peak-to-peak amplitude, which elicits saccadic bar pursuit triggered by super-threshold integrated error, 15 which, when averaged, tends to look like high-amplitude smooth tracking observed in prior work.<sup>27</sup>

In a separate series of experiments, we presented bar stimuli on a uniform, rather than a textured, background. For desert species, such a stimulus might more accurately represent common visual conditions. We tested bar widths that subtended between 7.5° and 120° on the retina (Figure S1A). We found that even the narrowest 7.5° bars elicited strong steering in desert flies, predicting at least 58% of the variability in the flies' steering responses (Figures S3B and S3C). By comparison, achieving a similar response in *D. melanogaster* required a 120° bar (Figure S3B). The r<sup>2</sup> values were larger for both *D. moj.* flies than for *D. melanogaster* for each bar width. To highlight this result,

we color-grouped linear fits across all bar widths for each species, showing that the correlation between stimulus and response was higher for desert species than *D. melanogaster* (Figure 3C).

Our initial intention was to incorporate the SoS stimulus into a systems identification approach to quantify the frequency tuning of object-tracking error across the different species. The assumptions of the analysis require linear relationships between the stimuli and the fly's responses. However, we discovered that desert flies produce many more body saccades than *D. melanogaster* (Figures 3D and 3E). Body saccades represent abrupt changes in flight heading that violate the assumption of stationarity, thereby precluding a linear systems analysis. For analysis of wide-field behavior, the comparatively fewer saccades can be filtered out without compromising a systems identification approach. <sup>28,29</sup> Due to the high rate of bar saccades, we therefore used the dynamically complex SoS stimulus for an unconstrained time-domain analysis.

We computationally isolated bar-evoked saccades and plotted trial-by-trial rasters (Figure 3D, top row) as well as binned probability histograms (Figure 3D, middle row). As expected, *D. melanogaster* executed saccades to track the bar (Figure 3Di). We were surprised to find that, in addition to increased smooth fixation by comparison with *D. melanogaster*, both desert fly species also performed bar-tracking saccades and did so at a significantly higher rate than *D. melanogaster* (Figures 3D and 3E). Across the three species, saccades were structured by the SoS dynamics, with "hot spots" in the saccade rasters coinciding with peaks in the velocity of the SoS stimulus after a short delay (Figure 3D, middle row), suggesting that velocity, possibly in addition to position, might be strong predictor of saccade triggering particularly in the *D. mojavensis* species (Figure 3D, bottom row).

In this study, we tested frontal centering and smooth fixation strategies among species occupying different visual ecological niches. Developing a predictive model of object-evoked saccades is beyond the scope of our efforts. However, upon noting the strong patterning of saccades, we performed a preliminary analysis to assess the proportion of variability in saccade execution that could be explained by the position and velocity of the SoS stimulus. We cross-correlated the stimulus position and velocity waveforms with saccade probability point-for-point in

#### Figure 3. D. mojavensis shows stronger smooth & saccadic responses to complex bar motion dynamics

(Ai) Left: individual responses (gray) to a motion-defined bar on a sum-of-sines motion trajectory (black) for 182 trials from n = 34 D. melanogaster flies. Colored trace represents the mean response. Right: exemplar trials from three different flies (gray) and the mean population response (green) overlaid with stimulus trace (black). Mean traces are lag-shifted and normalized to their own maximum values for visualization, which does not affect the correlation coefficients.

(Aii) Angular position of the stimulus plotted point-by-point against the mean response. The linear regression model fitted to the variables is plotted in black, with 95% confidence intervals in dashed gray. The coefficient of determination  $r^2$  is indicated on each plot.

- (B) Same as (A), but for 186 trials from n = 38 D. moj. baja.
- (C) Same as (A), but for 151 trials from n = 35 D. moj. moj.
- (Di) Top: raster plots indicating timing for 557 saccades from *D. melanogaster*. Middle: sliding saccade probability histograms are plotted below, signed to indicate direction. Bottom: onset-aligned bar angular position (black) and velocity (gray) are indicated.
- (Dii) Same as (Di), but for 1,691 saccades from *D. moj. baja*.
- (Diii) Same as (Di), but for 1,569 saccades from D. moj. moj.
- (Ei) Saccade rates separated by direction. Each dot indicates the average saccade rate during one trial. White horizontal lines indicate mean. Nonparametric Kruskal-Wallis tests  $^*p < 0.05$ ;  $^{**}p < 0.01$ ;  $^{***}p < 0.001$ .
- (Eii) Same as (Ei), but for counterclockwise saccades.
- (F) Linear regression as in (B), (D), and (F) for bar widths ranging from 7.5° to 120° color-grouped by species.

#### **Article**



time. In all three species, the maximum correlation coefficient occurred at negative time lag to the SoS position trace: *D. melanogaster* (–120 ms), *D. moj. baja* (–210 ms), and *D. moj. moj.* (–150 ms) (Figure S3). Thus, the saccades are triggered in advance of changes in bar position, making this variable a poor predictor of saccade probability—at least when considered on its own. By contrast, saccade probability lagged the stimulus velocity trace for *D. melanogaster* (270 ms), *D. moj. baja* (270 ms), and *D. moj. moj.* (330 ms). We found that bar velocity is a stronger predictor of saccades for *D. moj. baja* (41%) and *D. moj. moj.* (38%) than for *D. melanogaster* (14%) (Figures S3D–S3F). Further modeling efforts that might combine these variables are needed to describe the different strategies for saccadic object vision deployed by these fly species.

Although the average steering responses are smooth and highly correlated with the bar motion trajectory, the high saccade rates by desert flies make individual trials "jitter" around the SoS bar trajectory (Figures 3Bi and 3Ci, see individual traces). Thus, one could argue that the strategy used by the desert species is qualitatively similar to *D. melanogaster*—fixating the stationary ground and generating lots of small saccades to track the bar-rather than a contrasting strategy of smoothly fixating the bar and firing catch-up saccades. Resolving this issue is challenging with an SoS stimulus because it changes direction at random intervals, triggering more saccades in some intervals than others. In order to consistently sample inter-saccade bouts, we designed an experiment in which the bar revolved at a constant velocity, corresponding to the (70 °/s) velocity of each component sine wave in the previous experiment, for 10-s trials, in both clockwise (CW) (+) and counterclockwise (CCW) (-)

As previously demonstrated, 15 this experiment elicited bar pursuit characteristics in which D. melanogaster fixated the stationary ground in between bar-directed saccades, maintaining near-zero angular velocity during the inter-saccadic interval (ISI) (Figures 4Ai and 4Bi; Video S1). By contrast, and as predicted by the SoS results (Figure 3), D. moj. baja fixate the revolving bar in between saccades, not the stationary background, thus tracking the bar during the ISI with smooth pursuit (Figures 4Aii and 4Bii; Video S2). Similarly, D. moj. moj. fixate the bar during the ISI (Figures 4Aiii and 4Biii; Video S3). The distribution of ISI velocity values for D. melanogaster was skewed toward zero (Figure 4C, green), whereas both D. mojavensis subspecies' velocity distributions shifted toward the bar velocity (Figure 4C, orange & magenta). We compared the difference in means of ISI velocity across species and tested these differences with bootstrapped simulations, resampling with replacements from combined datasets, to find strong differences between species that are independent of stimulus direction (Figure 4D). In essence, we discovered that whereas D. melanogaster remains stationary, fixating the stationary ground in between saccades, D. moj. baja and D. moj. moj. continue moving to fixate the bar with interspersed saccades—a fixate-and-saccade tracking strategy.

These species differences in bar tracking are particularly noteworthy, given that the three flies smoothly track the oscillation of a wide-field ground at the driving frequency (Figures 2B and S2; Videos S4, S5, and S6) and between saccades show robust stimulus-matched optomotor fixation for a constant-velocity

wide-field ground (Figures S4B and S4C). However, the structure of wide-field optomotor saccades differs across species. In particular, *D. moj. moj.* shows erratic saccadic behavior, with individuals seeming to overshoot the stimulus rather than fixating it (Figure S4Aiii lower), and correspondingly high ISI velocity (Figure S4C). Accordingly, *D. moj. moj.* wide-field optomotor saccade dynamics are exaggerated in their amplitude, torque, and frequency compared with both *D. melanogaster* and *D. moj. baja* (Figures S4I–S4P). Whereas a deep analysis of wide-field optomotor behavior is beyond the scope of this study, it would seem that *D. moj. moj.* use underdamped optomotor control by comparison with *D. melanogaster*.<sup>30</sup>

#### D. mojavensis execute stronger, smaller, and morefrequent bar-tracking saccades than D. melanogaster

By contrast to the strong temporal patterning in response to the SoS stimulus (Figure 3D), the constant velocity bar produced evenly distributed tracking saccades by all three species (Figure 5A). As bar direction largely had no effect on saccade parameters within each species (Figures S4B-S4D), we combined CW and CCW saccades together to measure saccade-triggered average kinematic parameters. Previous work has shown that saccade dynamics can be tuned to characteristics of the visual stimulus (e.g., wide-field ground vs. small-field bars, low vs. high stimulus velocity). 15 Do saccade dynamics also vary across species? To address this question, we first measured the average trajectory of body position, velocity, acceleration, and torque for the three species (Figures 5B-5E). We found quantitative differences across species, even within D. mojavensis subspecies, for all kinematic variables that we tested (Figures 5F-5I). Both desert species produced lower-duration and more-frequent saccades than D. melanogaster (Figures 5G and 5I). D. moj. baja produced the most-frequent, smallest-amplitude, shortest, and slowest saccades. For the rest of the dynamics we quantified, we found differences both between D. melanogaster and each desert species and between the desert species themselves. D. moj. moj. saccades were larger in amplitude than D. moj. baja but smaller than D. melanogaster, though the latter difference was subtle and not statistically significant (Figure 5C). In D. moj. moj, these shorter and smaller saccades were achieved by increasing the torque produced by the animal, which resulted in higher acceleration and peak velocity during the body turn, and producing the braking countertorque earlier in the saccade profile than D. moj. baja. (Figures 5D and 5E). Overall, these varying dynamics support the hypothesis that, in addition to engaging smooth pursuit for object motion, specialist desert species trigger bar-directed saccades more frequently and modulate them to be smaller, shorter, and executed with higher torque than D. melanogaster.

#### **DISCUSSION**

This study tested the hypothesis that *Drosophila* species that have differing visual ecology employ divergent visual flight control strategies. *D. mojavensis* and *D. yakuba* are separated by 40 million years of divergence, <sup>31</sup> yet occupy similar visually sparse arid habitats. <sup>32</sup> When these flies are flown in an arena that allows free steering in the yaw plane, both species respond to a bar moving across a stationary background by employing a



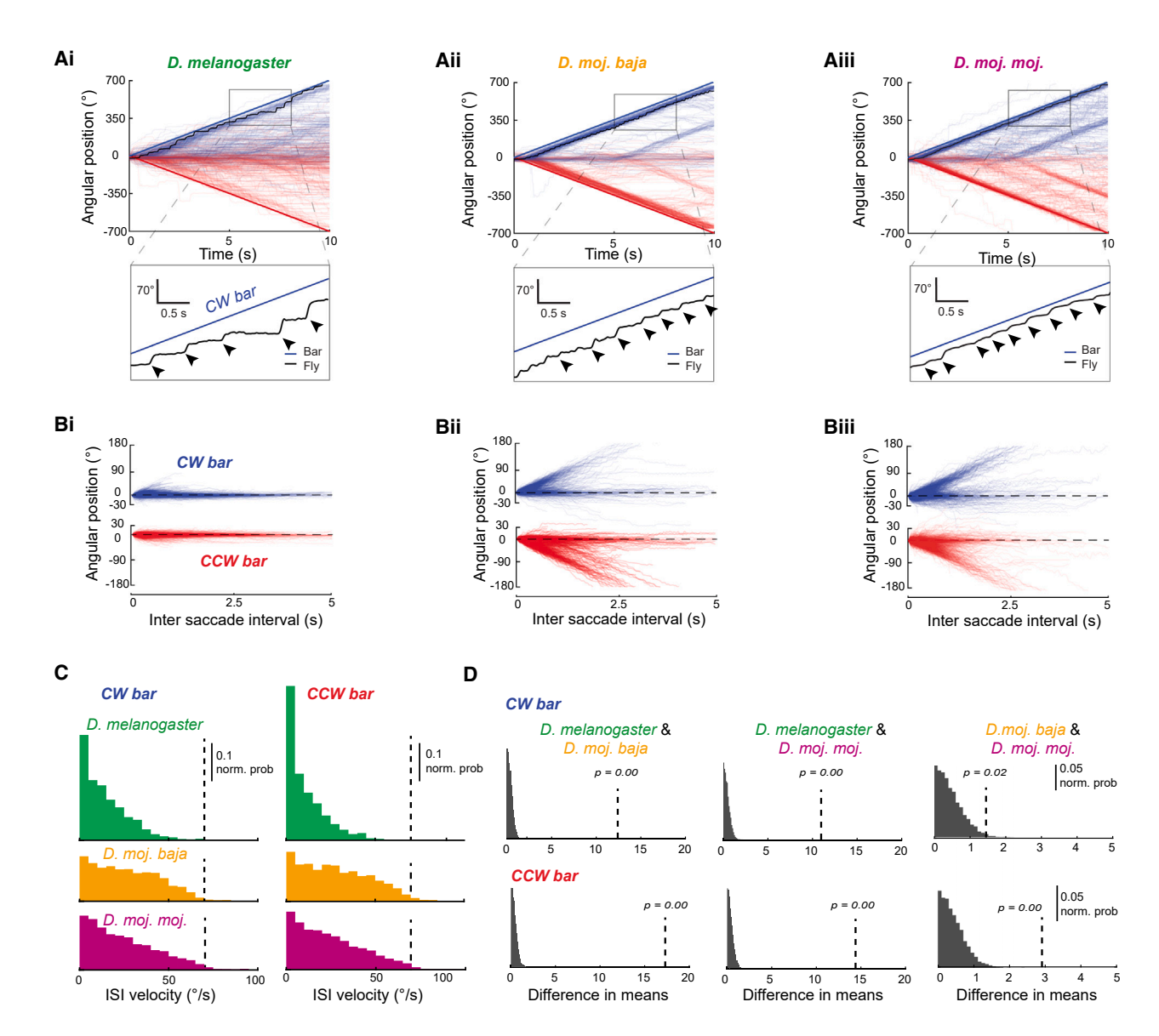


Figure 4. Steady state bar pursuit dynamics differ across species

(Ai) Individual unwrapped traces of pursuit of a revolving bar for n = 519 trials from N = 48 D. melanogaster, separated by bar direction. Bar trajectory is indicated with thick solid lines. An example trace is highlighted in black, with the inset. Black arrowheads indicate saccades.

- (Aii) Same as (Ai), but for 425 trials from  $n=45 \, D. \, moj. \, baja.$
- (Aiii) Same as (Ai), but for 461 trials from n = 48 D. moj. moj.
- (Bi) Inter-saccade flight bouts, grouped by stimulus direction, from  $\it D.~melanogaster.$
- (Bii) Same as (Bi), but from *D. moj. baja*.
- (Biii) Same as (Bi), but from D. moj. moj.
- (C) Normalized probability histograms of the mean angular velocity during inter-saccade bouts, grouped by stimulus direction. Vertical dashed line indicates the velocity of the bar.

(D) Paired comparisons of inter-saccade velocity across species. Probability histograms depict the distribution of 10,000 bootstrapped differences in means (bin size = 0.1), the dashed vertical line indicates the observed difference in means. p is the proportion of sampled differences in means equal to or greater than the observed difference in means.

See also Figure S4 and Videos S1, S2, S3, S4, S5, and S6.

fixate-and-saccade strategy characterized by smooth fixation dynamics and saccades to track the bar. By contrast, three different *D. melanogaster* strains, which occupy visually cluttered cosmopolitan human commensal habitats, smoothly fixate the background, not the bar, and orient toward the bar with saccades that override smooth ground fixation. Importantly, and in

stark contrast to *D. melanogaster*, we found that in desert species, flight bouts in between saccades are dominated by high-gain smooth object tracking. Thus, desert flies suppress the wide-field optomotor reflex that is so prominent in *D. melanogaster* in favor of fixating small-field object motion. Two closely related species of the melanogaster subgroup that

# **Current Biology Article**



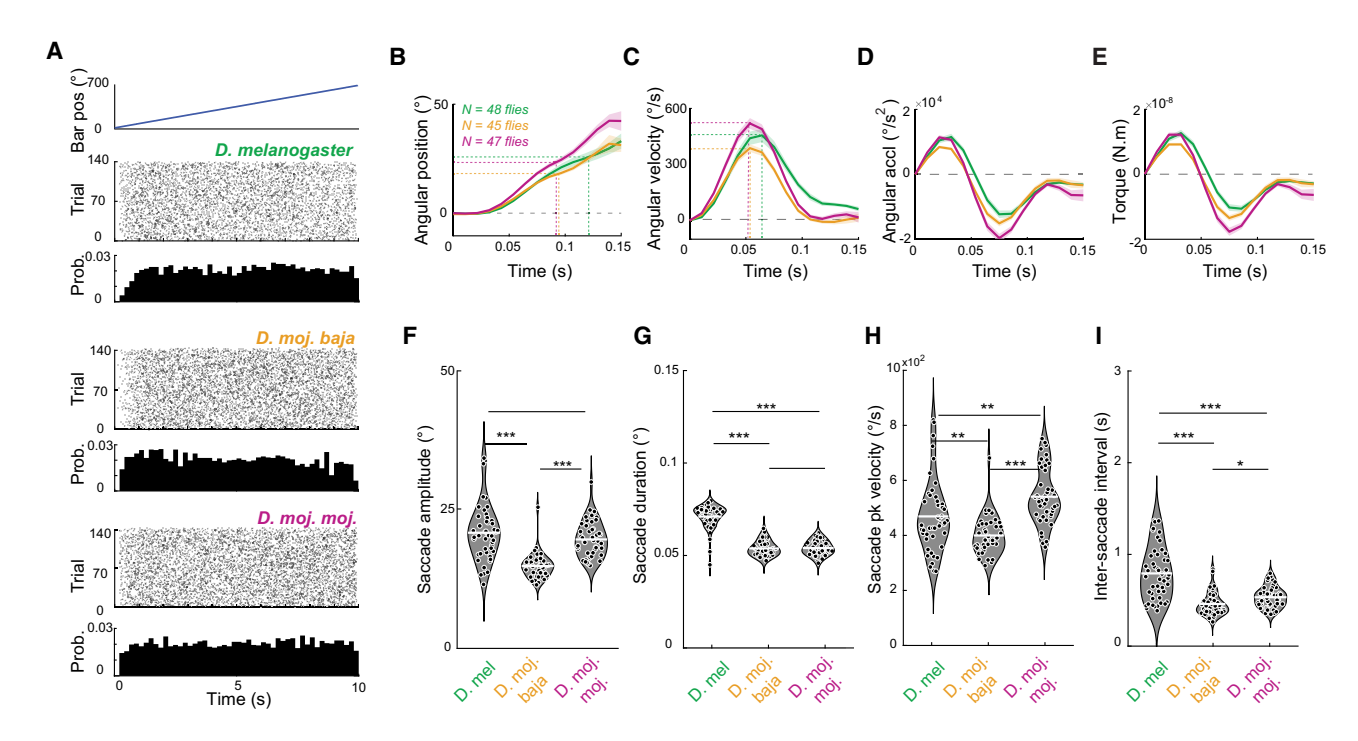


Figure 5. Object saccade dynamics differ across subspecies

(A) Top: angular position of a motion-defined bar during a 10-s CW revolution trial. Raster plot of saccades triggered by revolving bar for n = 48 D. melanogaster with corresponding normalized probability histogram (bin size = 200 ms). Below are corresponding raster plots and probability histograms for D. moj. baja (n = 45 flies) and D. moj. moj. (n = 47 flies).

(B) Change in body heading during a saccade, normalized to body angle position at saccade onset. Shaded color envelope indicates 95% confidence intervals. Dotted x intercepts indicate the time end point of the saccade and y intercepts the corresponding angular position at the end of the saccade (details for saccade identification in STAR Methods). Shaded envelopes represent standard deviation of mean.

- (C) Same as (B) for angular velocity. The peak velocities and the time points at which they occurred are indicated using dotted lines.
- (D) Same as (B) for saccade acceleration.
- (E) Same as (B) for saccade torque.
- (F) Comparison of saccade amplitude across species. Dots signify trial means from individual flies, white horizontal bars indicate population means. Nonparametric Kruskal-Wallis test p < 0.05; \*\*p < 0.01; \*\*p < 0.001.
- (G) Same as (F) for saccade duration.
- (H) Same as (F) for saccade peak velocity.
- (I) Same as (F) for inter-saccadic interval (ISI), which is inversely proportional to saccade frequency.

See also Figures S4 and S5.

have divergent visual ecologies employ different tracking strategies, supporting the hypothesis that visual flight control strategies are better fit to visual ecology than phylogeny.

## Inner-loop optomotor responses in flies are flexible and differentially tuned across drosophilids

Visual flight control in insects is achieved using two prominent visual behaviors: smooth gaze stabilization and saccades, the combination of which manifest as segments of straight flight interspersed with re-orientation body saccades. Straight flight is maintained by optomotor movements of the head and body that actively reduce retinal slip, keeping the image of the panorama fixated on the retina to counteract perturbations. This reflex is a low level "inner-loop" control process<sup>33</sup> that utilizes not only movements tuned to match image velocity but also fast catch-up or nystagmus saccades when the retinal slip velocity exceeds an error threshold. <sup>15,34,35</sup> Layered on top of this process, an "outer" control loop initiates body saccades that rapidly re-orient the animal, either to refresh the visual scene in the case of

spontaneous exploration<sup>36</sup> or to orient toward objects of ecological relevance.<sup>11</sup>

Visual signals for inner-loop optomotor reflexes are provided by directionally selective motion detectors T4/T5, which are small-field columnar neurons that are required for normal optomotor behavior,<sup>37</sup> which supply the wide-field dendrites of lobula plate tangential (LPT) cells. LPTs, in turn, supply select premotor descending neurons that trim optomotor responses to maintain stable visual orientation. 38,39 While high-gain inner-loop control provides robust stability to maintain course control and stable visual gaze, these reflexes are somewhat plastic. Looming circuits are differentially gated by the onset of flight and walking 40,41 and the amplitude of visual responses of the vertical system (VS) class of LPTs doubles, presumably to support the transition to high-velocity optic flow. 42,43 To voluntarily change course, outer-loop initiation of turns transiently hyperpolarizes LPTs that presumably assist optomotor equilibrium. 44,45 Stabilization reflexes must also be sensitive to multisensory modulation cues. In response to an attractive odorant, the gain of optomotor





responses transiently increases, <sup>42,43</sup> as do the visual responses of at least one LPT class. <sup>46</sup> Within the mechanosensory modality, proprioceptive feedback driven by active body movement has been shown to actively dampen optomotor responses. <sup>12,21</sup> Conversely, the onset of walking excites horizontal system (HS) even in the absence of visual input. <sup>47,48</sup>

Plasticity of optomotor control provides the premise that the switch from saccade-only bar tracking in *D. melanogaster* to smooth tracking observed in *D. mojavensis* is mediated by tuning the inner-loop optomotor controller (Figures 3A–3C and 4B). If so, then the correlation between the fly's steering response and the smooth variation in our SoS bar stimulus ought to be consistently higher for *D. mojavensis* than for *D. melanogaster*, which was indeed the case for experiments that varied bar width (Figures 3F, S3B, and S3C). These results expand the concept of flexible optomotor control for object tracking within multisensory and comparative contexts.

## Small-field optomotor responses support bar tracking and centering in desert flies

The robust smooth optomotor steering responses to frontal bar oscillation that we observed in both yaw-free *D. mojavensis* flies (Figures 2B–2D) and *D. yakuba* (Figures S2B and S2C) are similar to the responses to wide-field ground motion (Figure S2D). They are also similar to small-field responses observed in body-fixed, proprioception-compromised *D. melanogaster* for the same stimuli. Asymmetric smooth optomotor responses, larger for front-to-back object movement than back-to-front, are thought to mediate frontal bar centering under virtual closed-loop conditions in rigidly tethered flies. 37,50

High-gain bar optomotor responses accompany object centering in both yaw-free *D. mojavensis* (Figures 1Cii and 1Ciii) and *D. yakuba* (Figure S1C) but not in *D. melanogaster* strains (Figures S1 and S2). In *D. melanogaster*, optomotor responses are believed to be gated or attenuated by active damping, presumably via proprioceptive mechanoreceptors that rapidly signal body dynamics under yaw-free and free-flight conditions.<sup>21</sup> The physiological mechanisms for active damping remain to be revealed; our results suggest that visual responses are underdamped for habitats containing fewer optic flow cues.

However, smooth optomotor responses are not required for frontal centering—saccadic tracking can also suffice, as evidenced by Oregon-R and Canton-S (Figure S1B). Under yaw-free conditions with constant velocity bar motion, *D. melanogaster DL* have been shown to fixate the wide-field panorama to maintain stable gaze, while spatiotemporally integrating the angular position error to a threshold of roughly 2° s as the bar moves away from visual midline. <sup>15</sup> All three lab strains of *D. melanogaster* tested here orient toward the oscillating bar using saccades (Figure S2). All three also show robust ground fixation (Figure S2), so it seems most probable that the overall bartracking strategy and circuitry is conserved across strains, whereas the error threshold for triggering a saccade varies.

By comparison with T4/T5-based inner-loop optomotor control, the mechanistic basis of saccadic outer-loop object orientation is less well understood. Small-field T3 columnar neurons have been recently shown to be omnidirectional feature detectors, <sup>51</sup> which are robustly activated by the motion-defined bars that elicit object tracking, and must be functional for normal

saccadic bar-tracking flight behavior.<sup>14</sup> T3-analogous function remains to be explored in *D. mojavensis* or any other species, but two key control parameters are: (1) object pursuit is strongly saccadic but, unlike in *D. melanogaster*, (2) is ostensibly triggered by the tracking error between smooth fixation kinematics and bar velocity (Figures 3D, 3E, S3E, and S3F).

#### Visual ecology drives object-pursuit strategies

Animals across phyla show some combination of smooth and saccadic visual object pursuit,52 and canonical models for saccadic object pursuit in animals as diverse as primates and beetles incorporate both velocity and positional error components to trigger saccades. 52-54 In fact, within a single animal, the spatial composition of the visual background can modulate the balance of smooth and saccadic object pursuit. For example, in the praying mantis, a cluttered visual background influences the animal's target pursuit strategy; for a prey-like target superimposed upon a uniform grayscale background, their head/eye movements pursue the target smoothly, whereas the same target stimulus superimposed upon a natural cluttered background image causes a switch to saccadic target pursuit. The higher the contrast of the background, the longer the duration of stationary fixation bouts between saccades. 55 The interpretation is that the stationary visual background elicits bouts of gaze fixation via smooth optomotor control, while the object position error is integrated to saccade threshold (like D. melanogaster). Similarly, D. melanogaster on a magnetic tether smoothly pursues a bar if it is presented against a visually uniform grayscale background (albeit with lower gain than when body-fixed), whereas pursuit is saccadic against a naturally textured background. 15,21 This highlights the interplay between the demands of gaze stabilization and object pursuit.

Both the Mojave desert (*D. mojavensis*) and African savannah (*D. yakuba*) lack canopy cover, with broad, open woodland-grassland landscapes containing widely spaced trees. Two fly species—separated by 40 million years of divergence—that share this visual ecology may have evolved a fixed "clutterless" pursuit strategy, differing from *D. melanogaster*. Other object behaviors differ across *drosophilids* as well. For example, tall vertical objects are attractive and short objects aversive for *D. melanogaster*, <sup>56</sup> while *D. moj. moj.* robustly approach objects of any size. <sup>20</sup> It seems that, in order to overcome the challenges of a sparse visual environment, the visual control strategies of *D. moj. baja*, *D. moj. moj.*, and *D. yakuba* are geared toward small-field stimuli—visual objects of any size serve both as landmarks and as cues to stabilize gaze.

Natural image projections across the dorso-ventral axis of the visual field vary considerably during flight. For example, hawkmoths show strong stabilizing optomotor reflexes in response to optic flow cues in the ventral (ground) and lateral visual field, but steer to follow the contour image of the canopy in the dorsal field of view. With a larger number of more tightly packed ommatidia, *D. mojavensis* possesses a larger visual sensory volume than *D. melanogaster*. As the horizon forms a prominent visual feature in desert landscapes, we might expect different functional adaptations across the elevational axis of the visual field, but this remains to be explored.

In conclusion, our results reiterate that *D. melanogaster* uses a hybrid ground-fixate and object-saccade strategy, whereas

#### **Article**



*D. mojavensis* species use a fused fixate-and-saccade strategy for both ground-based gaze stabilization and orientation toward landscape features. We postulate that divergent visual ecology (Figure 1A) supports these distinct strategies. If so, what are the neural mechanisms that drive these adaptations? The availability of whole genomes and recent development of genetic tools for several drosophilids adapted to different ecologies presents a unique opportunity for comparative neuroethological studies that build upon deep understanding of *D. melanogaster* circuitry to explore mechanistic principles for ecological specializations. <sup>31,59,60</sup>

#### **RESOURCE AVAILABILITY**

#### **Lead contact**

Further information and requests for resources and reagents should be directed to and will be fulfilled by the lead contact, Mark Frye (frye@ucla.edu).

#### **Materials availability**

This study did not generate new unique reagents.

#### **Data and code availability**

All original code has been deposited at OSF and is publicly available as of the date of publication. OSF Data: https://osf.io/h74fn/. Any additional information required to reanalyze the data reported in this paper is available from the lead contact upon request.

#### **ACKNOWLEDGMENTS**

This work is funded by National Institutes of Health R01EY026031 and US Air Force Office of Scientific Research FA9550-23-1-0401 to M.A.F. and National Science Foundation IOS-2016188 to S.M.W. We thank Dr. Jean-Michel Mongeau for insight on frequency domain analysis. We thank Giulia Pelligrini for assistance with supplemental information collection.

#### **AUTHOR CONTRIBUTIONS**

M.R. conceptualized the project and contributed to methodology, investigation, software, formal analysis, visualization, writing the original draft, and editing. D.L. contributed to investigation and editing. S.M.W. contributed to conceptualization, funding acquisition, and editing. M.A.F. conceptualized the project and contributed to methodology, funding acquisition, supervision, project administration, writing the original draft, and editing.

#### **DECLARATION OF INTERESTS**

The authors declare no competing interests.

#### **STAR**\***METHODS**

Detailed methods are provided in the online version of this paper and include the following:

- KEY RESOURCES TABLE
- EXPERIMENTAL MODEL AND SUBJECT DETAILS
- METHOD DETAILS
  - Animal preparation
  - Magnetic tether experimental protocol
  - Visual stimuli
- QUANTIFICATION AND STATISTICAL ANALYSIS

#### SUPPLEMENTAL INFORMATION

Supplemental information can be found online at https://doi.org/10.1016/j.cub.2024.08.036

Received: April 16, 2024 Revised: July 29, 2024 Accepted: August 20, 2024 Published: September 17, 2024

#### **REFERENCES**

- Egelhaaf, M. (1987). Dynamic properties of two control systems underlying visually guided turning in house-flies. J. Comp. Physiol. 161, 777–783. https://doi.org/10.1007/BF00610219.
- Götz, K.G. (1968). Flight control in Drosophila by visual perception of motion. Kybernetik 4, 199–208. https://doi.org/10.1007/BF00272517.
- Cellini, B., and Mongeau, J.-M. (2020). Hybrid visual control in fly flight: insights into gaze shift via saccades. Curr. Opin. Insect Sci. 42, 23–31. https://doi.org/10.1016/j.cois.2020.08.009.
- Borst, A. (2014). Fly visual course control: behaviour, algorithms and circuits. Nat. Rev. Neurosci. 15, 590–599. https://doi.org/10.1038/nrn3799.
- Currier, T.A., Pang, M.M., and Clandinin, T.R. (2023). Visual processing in the fly, from photoreceptors to behavior. Genetics 224, iyad064. https://doi.org/10.1093/genetics/iyad064.
- Shinomiya, K., Nern, A., Meinertzhagen, I.A., Plaza, S.M., and Reiser, M.B. (2022). Neuronal circuits integrating visual motion information in Drosophila melanogaster. Curr. Biol. 32, 3529–3544.e2. https://doi.org/ 10.1016/j.cub.2022.06.061.
- Lachaise, D., Cariou, M.-L., David, J.R., Lemeunier, F., Tsacas, L., and Ashburner, M. (1988). Historical Biogeography of the Drosophila melanogaster Species Subgroup. In Evolutionary Biology, M.K. Hecht, B. Wallace, and G.T. Prance, eds. (Springer), pp. 159–225.
- David, J.R., and Capy, P. (1988). Genetic variation of Drosophila melanogaster natural populations. Trends Genet. 4, 106–111. https://doi.org/10.1016/0168-9525(88)90098-4.
- Atkinson, W., and Shorrocks, B. (1977). Breeding site specificity in the domestic species of Drosophila. Oecologia 29, 223–232. https://doi.org/10.1007/BF00345697.
- Markow, T.A. (2015). The secret lives of Drosophila flies. eLife 4, e06793. https://doi.org/10.7554/eLife.06793.
- van Breugel, F., and Dickinson, M.H. (2012). The visual control of landing and obstacle avoidance in the fruit fly Drosophila melanogaster. J. Exp. Biol. 215, 1783–1798. https://doi.org/10.1242/jeb.066498.
- Mongeau, J.-M., Cheng, K.Y., Aptekar, J., and Frye, M.A. (2019). Visuomotor strategies for object approach and aversion in Drosophila melanogaster. J. Exp. Biol. 222, jeb193730. https://doi.org/10.1242/jeb. 193730.
- Busch, C., Borst, A., and Mauss, A.S. (2018). Bi-directional Control of Walking Behavior by Horizontal Optic Flow Sensors. Curr. Biol. 28, 4037–4045.e5. https://doi.org/10.1016/j.cub.2018.11.010.
- Frighetto, G., and Frye, M.A. (2023). Columnar neurons support saccadic bar tracking in Drosophila. eLife 12, e83656. https://doi.org/10.7554/eLife. 83656.
- Mongeau, J.-M., and Frye, M.A. (2017). Drosophila Spatiotemporally Integrates Visual Signals to Control Saccades. Curr. Biol. 27, 2901– 2914.e2. https://doi.org/10.1016/j.cub.2017.08.035.
- Smith, G., Lohse, K., Etges, W.J., and Ritchie, M.G. (2012). Model-based comparisons of phylogeographic scenarios resolve the intraspecific divergence of cactophilic Drosophila mojavensis. Mol. Ecol. 21, 3293–3307. https://doi.org/10.1111/j.1365-294X.2012.05604.x.
- Throckmorton, L.H. (1975). The Phylogeny, Ecology & Geography of Drosophila. In Handbook of Genetics, R.C. King, ed. (Zenodo), pp. 421–469.
- Date, P., Crowley-Gall, A., Diefendorf, A.F., and Rollmann, S.M. (2017).
  Population differences in host plant preference and the importance of yeast and plant substrate to volatile composition. Ecol. Evol. 7, 3815–3825. https://doi.org/10.1002/ece3.2993.





- Heed, W.B. (1982). Ecological genetics and evolution: The cactus-yeastdrosophila model system, B.J. Stuart Flinton, and W.T. Starmer, eds. (Academic Press).
- Park, E.J., and Wasserman, S.M. (2018). Diversity of visuomotor reflexes in two Drosophila species. Curr. Biol. 28, R865–R866. https://doi.org/10. 1016/j.cub.2018.06.071.
- Rimniceanu, M., Currea, J.P., and Frye, M.A. (2023). Proprioception gates visual object fixation in flying flies. Curr. Biol. 33, 1459–1471.e3. https://doi.org/10.1016/j.cub.2023.03.018.
- Götz, K.G. (1987). Course-Control, Metabolism and Wing Interference During Ultralong Tethered Flight in Drosophila Melanogaster. J. Exp. Biol. 128, 35–46. https://doi.org/10.1242/jeb.128.1.35.
- 23. Heisenberg, M., and Wolf, R. (1984). Vision in Drosophila: Genetics of Microbehavior (Springer-Verlag).
- Greenspan, R.J., and Ferveur, J.F. (2000). Courtship in Drosophila. Annu. Rev. Genet. 34, 205–232. https://doi.org/10.1146/annurev.genet.34. 1.205.
- Duistermars, B.J., Reiser, M.B., Zhu, Y., and Frye, M.A. (2007). Dynamic properties of large-field and small-field optomotor flight responses in Drosophila. J. Comp. Physiol. A Neuroethol. Sens. Neural Behav. Physiol. 193, 787–799. https://doi.org/10.1007/s00359-007-0233-y.
- Roth, E., Zhuang, K., Stamper, S.A., Fortune, E.S., and Cowan, N.J. (2011). Stimulus predictability mediates a switch in locomotor smooth pursuit performance for Eigenmannia virescens. J. Exp. Biol. 214, 1170–1180. https://doi.org/10.1242/jeb.048124.
- Theobald, J.C., Duistermars, B.J., Ringach, D.L., and Frye, M.A. (2008).
  Flies see second-order motion. Curr. Biol. 18, R464–R465. https://doi.org/10.1016/j.cub.2008.03.050.
- Cellini, B., and Mongeau, J.-M. (2020). Active vision shapes and coordinates flight motor responses in flies. Proc. Natl. Acad. Sci. USA 117, 23085–23095. https://doi.org/10.1073/pnas.1920846117.
- Cellini, B., Salem, W., and Mongeau, J.-M. (2022). Complementary feed-back control enables effective gaze stabilization in animals. Proc. Natl. Acad. Sci. USA 119, e2121660119. https://doi.org/10.1073/pnas. 2121660119.
- Cellini, B., and Mongeau, J.-M. (2022). Nested mechanosensory feedback actively damps visually guided head movements in Drosophila. eLife 11, e80880. https://doi.org/10.7554/eLife.80880.
- Drosophila 12 Genomes Consortium, Clark, A.G., Eisen, M.B., Smith, D.R., Bergman, C.M., Oliver, B., Markow, T.A., Kaufman, T.C., Kellis, M., Gelbart, W., et al. (2007). Evolution of genes and genomes on the Drosophila phylogeny. Nature 450, 203–218. https://doi.org/10.1038/ nature06341.
- Oliveira, D.C.S.G., Almeida, F.C., O'Grady, P.M., Armella, M.A., DeSalle, R., and Etges, W.J. (2012). Monophyly, divergence times, and evolution of host plant use inferred from a revised phylogeny of the Drosophila repleta species group. Mol. Phylogenet. Evol. 64, 533–544. https://doi.org/ 10.1016/j.ympev.2012.05.012.
- Hardcastle, B.J., and Krapp, H.G. (2016). Evolution of Biological Image Stabilization. Curr. Biol. 26, R1010–R1021. https://doi.org/10.1016/j.cub. 2016.08.059.
- Davis, B.A., and Mongeau, J.-M. (2023). The influence of saccades on yaw gaze stabilization in fly flight. PLoS Comput. Biol. 19, e1011746. https:// doi.org/10.1371/journal.pcbi.1011746.
- Cellini, B., Salem, W., and Mongeau, J.-M. (2021). Mechanisms of punctuated vision in fly flight. Curr. Biol. 31, 4009–4024.e3. https://doi.org/10.1016/j.cub.2021.06.080.
- Ros, I.G., Omoto, J.J., and Dickinson, M.H. (2024). Descending control and regulation of spontaneous flight turns in Drosophila. Curr. Biol. 34, 531–540.e5. https://doi.org/10.1016/j.cub.2023.12.047.
- Fenk, L.M., Poehlmann, A., and Straw, A.D. (2014). Asymmetric Processing of Visual Motion for Simultaneous Object and Background Responses. Curr. Biol. 24, 2913–2919. https://doi.org/10.1016/j.cub. 2014.10.042

- 38. Palmer, E.H., Omoto, J.J., and Dickinson, M.H. (2022). The role of a population of descending neurons in the optomotor response in flying Drosophila. Preprint at bioRxiv.
- 39. Isaacson, M.D., Eliason, J.L.M., Nern, A., Rogers, E.M., Lott, G.K., Tabachnik, T., Rowell, W.J., Edwards, A.W., Korff, W.L., Rubin, G.M., et al. (2023). Small-field visual projection neurons detect translational optic flow and support walking control. Preprint at bioRxiv.
- Ache, J.M., Namiki, S., Lee, A., Branson, K., and Card, G.M. (2019). State-dependent decoupling of sensory and motor circuits underlies behavioral flexibility in Drosophila. Nat. Neurosci. 22, 1132–1139. https://doi.org/10.1038/s41593-019-0413-4.
- Ache, J.M., Polsky, J., Alghailani, S., Parekh, R., Breads, P., Peek, M.Y., Bock, D.D., von Reyn, C.R., and Card, G.M. (2019). Neural Basis for Looming Size and Velocity Encoding in the Drosophila Giant Fiber Escape Pathway. Curr. Biol. 29, 1073–1081.e4. https://doi.org/10.1016/ i.cub.2019.01.079.
- Chow, D.M., and Frye, M.A. (2008). Context-dependent olfactory enhancement of optomotor flight control in D.melanogaster. J. Exp. Biol. 211, 2478–2485. https://doi.org/10.1242/jeb.018879.
- Chow, D.M., Theobald, J.C., and Frye, M.A. (2011). An olfactory circuit increases the fidelity of visual behavior. J. Neurosci. 31, 15035–15047. https://doi.org/10.1523/JNEUROSCI.1736-11.2011.
- Kim, A.J., Fitzgerald, J.K., and Maimon, G. (2015). Cellular evidence for efference copy in Drosophila visuomotor processing. Nat. Neurosci. 18, 1247–1255. https://doi.org/10.1038/nn.4083.
- Fenk, L.M., Kim, A.J., and Maimon, G. (2021). Suppression of motion vision during course-changing, but not course-stabilizing, navigational turns. Curr. Biol. 31, 4608–4619.e3. https://doi.org/10.1016/j.cub.2021. 09.068.
- Wasserman, S.M., Aptekar, J.W., Lu, P., Nguyen, J., Wang, A.L., Keles, M.F., Grygoruk, A., Krantz, D.E., Larsen, C., and Frye, M.A. (2015).
   Olfactory Neuromodulation of Motion Vision Circuitry in Drosophila. Curr. Biol. 25, 467–472. https://doi.org/10.1016/j.cub.2014.12.012.
- Fujiwara, T., Cruz, T.L., Bohnslav, J.P., and Chiappe, M.E. (2017). A faithful internal representation of walking movements in the Drosophila visual system. Nat. Neurosci. 20, 72–81. https://doi.org/10.1038/nn.4435.
- Fujiwara, T., Brotas, M., and Chiappe, M.E. (2022). Walking strides direct rapid and flexible recruitment of visual circuits for course control in Drosophila. Neuron 110, 2124–2138.e8. https://doi.org/10.1016/j. neuron 2022 04 008
- Theobald, J.C., Shoemaker, P.A., Ringach, D.L., and Frye, M.A. (2010).
  Theta motion processing in fruit flies. Front. Behav. Neurosci. 4, 35. https://doi.org/10.3389/fnbeh.2010.00035.
- Fox, J.L., Aptekar, J.W., Zolotova, N.M., Shoemaker, P.A., and Frye, M.A. (2014). Figure-ground discrimination behavior in Drosophila. I. Spatial organization of wing-steering responses. J. Exp. Biol. 217, 558–569. https://doi.org/10.1242/jeb.097220.
- Keleş, M.F., Hardcastle, B.J., Städele, C., Xiao, Q., and Frye, M.A. (2020).
  Inhibitory interactions and columnar inputs to an object motion detector in Drosophila. Cell Rep. 30, 2115–2124.e5. https://doi.org/10.1016/j.celrep. 2020.01.061
- Land, M.F. (1992). Visual tracking and pursuit: humans and arthropods compared. J. Insect Physiol. 38, 939–951. https://doi.org/10.1016/0022-1910(92)90002-U.
- Lisberger, S.G., Morris, E.J., and Tychsen, L. (1987). Visual motion processing and sensory-motor integration for smooth pursuit eye movements. Annu. Rev. Neurosci. 10, 97–129. https://doi.org/10.1146/annurev.ne.10.030187.000525.
- Talley, J., Pusdekar, S., Feltenberger, A., Ketner, N., Evers, J., Liu, M., Gosh, A., Palmer, S.E., Wardill, T.J., and Gonzalez-Bellido, P.T. (2023).
   Predictive saccades and decision making in the beetle-predating saffron robber fly. Curr. Biol. 33, 2912–2924.e5. https://doi.org/10.1016/j.cub. 2023.06.019.

# **Current Biology**Article



- Rossel, S. (1980). Foveal fixation and tracking in the praying mantis.
  J. Comp. Physiol. 139, 307–331. https://doi.org/10.1007/BF00610462.
- Maimon, G., Straw, A.D., and Dickinson, M.H. (2008). A simple vision-based algorithm for decision making in flying Drosophila. Curr. Biol. 18, 464–470. https://doi.org/10.1016/j.cub.2008.02.054.
- Bigge, R., Pfefferle, M., Pfeiffer, K., and Stöckl, A. (2021). Natural image statistics in the dorsal and ventral visual field match a switch in flight behaviour of a hawkmoth. Curr. Biol. 31, R280–R281. https://doi.org/10. 1016/j.cub.2021.02.022.
- Currea, J.P., Frazer, R., Wasserman, S.M., and Theobald, J. (2022). Acuity and summation strategies differ in vinegar and desert fruit flies. iScience 25, 103637. https://doi.org/10.1016/j.isci.2021.103637.
- Stern, D.L. (2022). Transgenic tools for targeted chromosome rearrangements allow construction of balancer chromosomes in non-melanogaster Drosophila species. G3 (Bethesda) 12, jkac030. https://doi.org/10.1093/g3journal/jkac030.
- Coleman, R.T., Morantte, I., Koreman, G.T., Cheng, M.L., Ding, Y., and Ruta, V. (2023). A modular circuit architecture coordinates the

- diversification of courtship strategies in Drosophila. Preprint at bioRxiv. https://doi.org/10.1101/2023.09.16.558080.
- Bender, J.A., and Dickinson, M.H. (2006). Visual stimulation of saccades in magnetically tethered Drosophila. J. Exp. Biol. 209, 3170–3182. https://doi.org/10.1242/jeb.02369.
- Duistermars, B.J., and Frye, M. (2008). A magnetic tether system to investigate visual and olfactory mediated flight control in Drosophila. J. Vis. Exp. 21, 1063. https://doi.org/10.3791/1063.
- Stöckl, A.L., Kihlström, K., Chandler, S., and Sponberg, S. (2017).
  Comparative system identification of flower tracking performance in three hawkmoth species reveals adaptations for dim light vision. Philos. Trans. R. Soc. Lond. B Biol. Sci. 372.
- **64.** Roth, E., Sponberg, S., and Cowan, N.J. (2014). A comparative approach to closed-loop computation. Curr. Opin. Neurobiol. 25, 54–62.2.
- Berens, P. (2009). CircStat: A MATLAB Toolbox for Circular Statistics. J. Stat. Softw. 31, 1–21.





#### **STAR**\*METHODS

#### **KEY RESOURCES TABLE**

REAGENT or RESOURCE	SOURCE	IDENTIFIER
Electronic equipment		
LED panel visual display system	IO Rodeo	57
Neutral density filters	Rosco	Cat# 59
BlackFly USB camera	FLIR	BFS-U3-04S2M-CS
Data Acquisition Hardware	National Instruments	NI USB-6212
Experimental models: Organisms/strains		
Drosophila melanogaster Canton-S	Bloomington Drosophila Stock Center	Stock #33
Drosophila melanogaster Oregon-R	Bloomington Drosophila Stock Center	Stock #5
Drosophila melanogaster	Dickinson Lab	Dickinson Lab Flies (DL)
Drosophila mojavensis mojavensis	Garrity Lab	https://www.drosophilaspecies.com/
Drosophila mojavensis baja	Garrity Lab	https://www.drosophilaspecies.com/
Drosophila yakuba	Donlea Lab	https://www.drosophilaspecies.com/
Software and algorithms		
Data and plotting code	OSF	DOI https://doi.org/10.17605/OSF.IO/H74FN
MATLAB	MathWorks	http://www.mathworks.com/
Circular Statistics Toolbox	Philipp Berens	Currea et al. <sup>58</sup>
CircHeatMap	Joshua Welsh	https://github.com/joadwe/cirheatmap/releases/tag/v1.71

#### **EXPERIMENTAL MODEL AND SUBJECT DETAILS**

A wild-type *Drosophila melanogaster* strain was maintained at 25°C under a 12 hr: 12 hr light:dark cycle with access to food and water ad *libitum*. *D. mojavensis mojavensis* and *D. mojavensis baja* originated from the Garrity Lab at Brandeis University and were subsequently reared in laboratory conditions for 100+ generations under the same temperature, circadian and nutrition conditions as *D. melanogaster*. All behavioral experiments were performed with randomly selected 3-6 day-old female flies within 4 hours of lights on and 4 hours of lights off.

#### **METHOD DETAILS**

#### **Animal preparation**

We used a magnetic tether paradigm and prepared the animals for each experiment according to a protocol that has been previously described.  $^{21}$  Briefly, we cold-anesthetized the flies by cooling them on a Peltier stage maintained at approximately  $^4$ °C. We glued stainless steel minutien pins (Fine Science Tools, SKU 26002-10) onto the thorax by applying UV-activated glue (Esslinger, SKU 12.201). The pin's length was approximately 1 cm to minimize the moment arm about which the fly can generate cross-field torques in pitch and roll. The pins were less than 1 percent of the fly's moment of inertia about the yaw axis. The pin was placed on the thorax projecting forward at an angle of approximately  $30^\circ$ , in order to closely mimic the fly body's angle of attack during low velocity free flight. Before running experiments, flies were allowed at least half an hour and no longer than 2 hours to recover upside-down in a custom-designed holder, inside a covered acrylic container where humidity and temperature could be controlled in order to avoid rapid dehydration ( $\sim 24^\circ$ C, 50% humidity). After recovering from anesthesia, flies were given small pieces of Kimwipe as a proxy for a landing substrate to cling to and prevent flight and energy expenditure. It should be noted that *D. mojavensis* flies commonly released the Kimwipe and initiated flight whereas *D. melanogaster* more readily held on to the Kimwipe.

#### Magnetic tether experimental protocol

As previously described, <sup>61,62</sup> the magnetic-tether arena is comprised of a cylindrical display that consists of an array of 96 × 16 blue light emitting diodes (470 nm emission peak) that wrap around the fly, subtending 360° horizontally and 60° vertically (Figure 1B). Each singular LED subtends 3.75° on the flies' retina. Flies were suspended between two magnets, allowing free rotation along the vertical (yaw) axis. We illuminated the fly from above with an array of six infrared LEDs (940 nm emission peak) and visualized the fly's body from below using an infrared-sensitive camera (BlackFly BFS-U3-04S2M-CS) fitted with a zoom lens (InfiniStix 1.0x/94mm, Edmund Optics) and an 850 nm longpass filter (FGL850M, ThorLabs) to block light from the LED panels. We recorded

## **Current Biology**Article



the angular position of the fly within the arena at 100 frames/s. At the beginning of each experiment, we characterized flies average optomotor behavior by presenting a wide-field panorama rotating at 120°/s for 20 s in the CW and the CCW directions. Flies that did not complete this trial or displayed excessive wobble were discarded from the experiment. If a fly stopped flying during a trial, the experimenter blew a gentle puff of air to stimulate the fly to re-initiate flight. Only flies that flew continuously for at least 75% of the experimental trials were included in the analysis.

#### Visual stimuli

Experiments for Figures 1 and 2 were designed to test responses to constant velocity stimuli, thus containing power across frequencies. Trials lasted 4 s with 2-4 s rests between trials. Bar trials used a 30° wide textured bar on a textured background panorama. Motion-defined bars were used to elicit responses to object movement and minimize the influence of luminance contrast cues that might provoke static positional responses. Both the bar and the background were illuminated with a random pattern of bright and dark vertical stripes at maximum contrast subject to a spatial bandpass filter requiring most stripes to be between 1 and 3 pixels in width, and with an enforced 50% ON/OFF distribution of luminance values. A single set of background and bar patterns were used for all trials. In all cases, we presented objects on a spatially randomized static background scene to closely mimic spatially broadband panoramic visual landscapes. In each bar trial, bars were presented in one of 12 pseudorandomized evenly distributed azimuthal positions relative to the fly's heading. Bars were oscillated at 2 Hz on a triangle wave with 60° peak-to-peak amplitude moving at 120°/s. Ground trials where the whole panorama oscillated on the same motion trajectory were interleaved with bar trials as a positive control measurement of wide-field optomotor performance. Flies that did not show significant optomotor responses were discarded from the dataset. *D. mojavensis* retinal resolution is 0.13 cycles per degree, therefore can resolve 7.7 degree pattern wavelength. *D. melanogaster* resolution is 0.10 cycles per degree, therefore can resolve 10 degree pattern wavelength. The random patterns we use contain single wavelengths that intersperse stripes that vary from 2-6 pixels in width, corresponding to 7.5-22.5 degrees, providing good coverage of wavelength for both species.

As discussed in the main text, for Figure 3, we designed a complex motion trajectory for the same 30° motion-defined bar object with the intention of using a frequency-domain analysis to quantify the strength of bar-elicited smooth responses across several oscillation frequencies. In addition to representing more naturalistic complex motion dynamics, this method would have allowed us to assess the frequency tuning of smooth responses observed in *D. mojavensis*. Following the approach adopted by Stockl et al. 2017<sup>63</sup> to explore flower-tracking performance across hawkmoth species, this motion trajectory was the sum of nine sine waves (0.3 – 11.3 Hz) selected to be non-overlapping prime multiples (Roth et al. 2014, 64 Stockl et al. 2017<sup>63</sup>). Trials were 10 s in duration and consisted of either bar motion on this trajectory or, like the previous experiment, broadband ground motion on this same trajectory. For bar trials, the angular position of the fly was extracted from the video feed at the start of each trial and the stimulus was programmed to appear in the frontal field of view, +/- 60° from the longitudinal body axis.

Experiments for Figures 4 and 5 were designed to explore how and whether saccades and inter-saccadic flight bouts differ across species. To do this, we revolved the same 30° motion-defined bar around the visual arena at a constant velocity of 70°/s, with the broadband background kept stationary. This motion trajectory was specifically chosen to elicit continuous object pursuit and assess its smooth and saccadic components separately, as previously described. The bar again appeared on the fly's visual midline and revolved in randomly assigned CW and CCW directions for 10s trials, with 2-3 trials presented for each stimulus direction. These trials were again interleaved with trials where the broadband ground revolved on the same motion trajectories.

#### **QUANTIFICATION AND STATISTICAL ANALYSIS**

All heading angle extraction and statistical analyses were performed using MATLAB (MathWorks, Natick, MA, USA). All fly video data was recorded at 100 fps using a FLIR Blackfly camera (BFS-U3-04S2M-CS) and stimulus position data was recorded at 1000 fps using a National Instruments data acquisition board (NI USB-6212). Fly angular heading was extracted using custom-made algorithms that in part included training custom neural net classifiers using software provided by Dr. Ben Cellini (https://github.com/BenCellini/heading-detector-network). Post angular heading extraction, raw data was low-pass filtered using a 5<sup>th</sup> order Butterworth filter with a 20 Hz cutoff frequency. Clockwise (CW) was defined as the positive direction of motion throughout. Body saccades were extracted using peak-detection methods applied to body angular velocity as per, <sup>15</sup> with adjustments in some detection parameters in order to accurately identify all saccades across species. Inter-saccadic flight bouts of at least 0.2 s duration were isolated and used for subsequent analyses.

For raw object orientation responses in Figure 1, we constructed circular probability heat maps to represent the overall likelihood of flies orienting towards a specific angular heading relative to the bar. For each trial performed by an individual fly, a circular mean resultant heading vector  $\theta$  and resultant vector magnitude r were computed using a 50 ms scanning window. <sup>65</sup> r values represent the length of radii on a unit circle, and were therefore within the range of 0 to 1, with values closer to 1 representing less spread around the mean heading  $\theta$ . We computed the normalized probability of both angular heading  $\theta$  (bin width = 1°) and vector length r (bin width = 0.2) using the population dataset. We used the custom CircHeatmap function to represent the bivariate probability using a heat map (https://github.com/joadwe/cirheatmap).

For Figure 2, saccades were eliminated and inter-saccadic bouts were averaged within an individual fly to obtain a mean fly response. Fly means were averaged across the population for each dataset. Fast Fourier Transforms (FFTs) were performed for each individual fly and the amplitude of bar FFT for each fly was normalized to that fly's optomotor ground response. The magnitude





ratios at the relevant peaks were compared across species using unpaired samples Student's t-test. Unless otherwise specified, each dot in a scatter plot represents an individual fly's mean response.

For Figures 3 and S1, when a linear systems identification approach has been previously applied in flying fly paradigm assessing performance of the gaze stabilization optomotor reflex, the key assumption of linearity was satisfied by the removal of the occasional nonlinearity represented by a sudden high-velocity change in angular heading i.e. a saccade. <sup>28,29</sup> However, in our study, we were surprised to find that in addition to smooth dynamics, the object-tracking responses in *D. mojavensis* were also strongly saccadic, patterned with the SoS stimulus dynamics (Figure 3). Thus, a linear systems identification analysis was inappropriate to characterize the frequency tuning of smooth object responses in desert flies and we opted for an event-triggered time-domain analysis instead. Future studies might succeed with this method to characterize the frequency tuning of smooth object responses in desert flies by reducing the amplitude of object oscillation that triggers fewer saccades.

Here, we calculated the mean population response to the sum-of-sines stimulus and cross-correlated it with the stimulus trajectory to find the phase lag between the two signals. We then shifted the response by that lag and plotted the stimulus vs. response point-by-point. We tested the hypothesis that the fly's response is predicted by the stimulus trajectory by fitting a linear regression model to the data to determine the correlation coefficient (r), the coefficient of determination (r²) and 95 % confidence intervals. We were thus able to estimate how much of the variability in the fly's object tracking response, including both smooth and saccadic components, was predicted by the stimulus dynamics across the three species. Removing the phase lag changes the intercept of the linear fit, but not the correlation coefficient. We constructed raster plots indicating the timing of each saccade within the 10 s trial across all trials, and obtained normalized saccade probability histograms, for CW and CCW saccades, binned into 200 ms time windows.

To determine the predictive power of stimulus position and velocity on saccade probability, we first interpolated the normalized saccade probability, grouping CW and CCW saccades together, to obtain a smooth trace (Figure S2). We then rectified the position trace and from this signal obtained a rectified stimulus velocity trace by differentiating using a 20 ms sliding window. We cross-correlated the saccade probability with both stimulus position and with stimulus velocity to determine the phase lags of each. As previously described, we used the lag-shifted stimulus velocity trace to determine the predictive power of bar angular velocity on saccade probability.

For statistical analysis of inter-saccadic bouts used to track a revolving bar, we first computed the mean velocity of each tracking bout and represented them in normalized probability histograms using  $5^{\circ}$ /s bins. We then used a bootstrapping technique to test the null hypothesis that inter-saccadic bouts across species all originate from the same dataset. We performed pairwise analyses by combining bout velocities for two species at a time, sampling with replacement 10,000 times and compared the distribution of bootstrap sampled difference in means to the observed difference in means. p-values indicate the proportion of bootstrapped difference in means that is greater than the observed difference in means between species. Thus, for p = 0.01 would indicate that one percent of the possible differences that these data sets could produce would be further apart (less similar) than the differences we observed, whereas ninety nine percent would be closer together (more similar).

Saccade measurement variables including amplitude, duration, peak velocity and inter-saccadic intervals (ISIs) were extracted using previously described methods. <sup>15</sup> For plotting saccade kinematics, we normalized traces to saccade onset. We obtained angular velocity and acceleration through linear derivation and computed angular torque using a previously established model where. <sup>15</sup> Mean saccade metrics were calculated for all saccades performed by an individual fly throughout their experimental trials. Population means were calculated from these individual means. For revolving bar experiments, we used a bootstrapping analysis to show that CW and CCW saccade dynamics do not differ (Figure S4) and proceeded with the analysis on the combined directions dataset. We used non-parametric Kruskal-Wallis tests to compare dynamics across species with \*p < 0.05; \*\*p < 0.01; \*\*\*p < 0.001.